Earth Planets Space, **58**, 1349–1358, 2006

Paleomagnetism of the Pleistocene Tequila Volcanic Field (Western Mexico)

Maria Rodríguez Ceja[1], Avto Goguitchaichvili[1,2*] , Manuel Calvo-Rathert[3], Juan Morales-Contreras[1], Luis Alva-Valdivia[1], José Rosas Elguera[4], Jaime Urrutia Fucugauchi[1], and Hugo Delgado Granados[5]

[1]*Laboratorio de Paleomagnetismo, Instituto de Geofísica, Universidad Nacional Autónoma de México, Ciudad Universitaria s/n, 04510 D.F., México*
[2]*Laboratorio Interinstitucional de Magnetismo Natural, Instituto de Geofísica, Universidad Nacional Autónoma de México, Coeneo, Michoacán, México*
[3]*Dpto. de Física, E. P. S., Universidad de Burgos, Av. Cantabria, s/n, Burgos, Spain*
[4] *Centro de Ciencias de la Tierra, Universidad de Guadalajara, 44840 Guadalajara, México*
[5]*Departamento de Vulcanología, Instituto de Geofísica, Universidad Nacional Autónoma de México, Ciudad Universitaria s/n, 04510 D.F., México*

(Received November 30, 2005; Revised May 25, 2006; Accepted May 26, 2006; Online published November 8, 2006)

This paper presents new paleomagnetic results from 24 independent cooling units in Tequila area (western Trans-Mexican Volcanic Belt). These units were recently dated by means of state-of-the-art ^{40}Ar-^{39}Ar method (Lewis-Kenedy *et al*., 2005) and span from 1130 to 150 ka. The characteristic paleodirections are successfully isolated for 20 cooling units. The mean paleodirection, discarding intermediate polarity sites, is $I = 29.6^\circ$, $D = 359.2^\circ$, $k = 26$, $\alpha_{95} = 7.1^\circ$, $n = 17$, which corresponds to the mean paleomagnetic pole position $P_{\rm lat} = 85.8^\circ$, $P_{\rm long} = 84.3^\circ$, $K = 27.5$, $A_{95} = 6.9^\circ$. These directions are practically undistinguishable from the expected Plestocene paleodirections, as derived from reference poles for the North American polar wander curve and in agreement with previously reported directions from western Trans-Mexican Volcanic Belt. This suggests that no major tectonic deformation occurred in studied area since early-middle Plestocene to present. The paleosecular variation is estimated trough the study of the scatter of virtual geomagnetic poles giving $S_F = 15.4$ with $S_U = 19.9$ and $S_L = 12.5$ (upper and lower limits respectively). These values are consistent with those predicted by the latitude-dependent variation model of McFadden *et al*. (1991) for the last 5 Myr. The interesting feature of the paleomagnetic record obtained here is the occurrence of an intermediate polarity at 671 ± 13 ka which may correspond the worldwide observed Delta excursion at about 680–690 ka. This gives the volcanic evidence of this event. Two independent lava flows dated as 362 ± 13 and 354 ± 5 ka respectively, yield transitional paleodirections as well, probably corresponding to the Levantine excursion.

Key words: Paleomagnetism, rock-magnetism, paleosecular variation, magnetic stratigraphy, Western Mexico.

1. Introduction

The paleosecular variation (PSV) and reversals are two major features of the Earth's magnetic field. PSVs are manifested slowly through the years and are known from direct instrumental measurements since the 16th century, when observatory records initiated. Direct observations show that the direction and magnitude of the non-dipolar field is irregularly distributed over the Earth's surface; variation of the field is larger in the southern hemisphere than in the northern hemisphere, and completely lacking in the central Pacific Ocean region (Doell and Cox, 1972). In order to extend the knowledge of the paleosecular variation over time scales larger than observatory records two potential datasets may be used: paleomagnetic records obtained from sedimentary and volcanic rocks of known age. Sediments can provide semi-continuous records of magnetic field variation, but problems with remanence acquisition mechanism and diagenetic process may affect the signal. Data obtained from lavas, while providing spot readings, are not subject to the controversies over reliability that make interpretation of sedimentary data so difficult (Tauxe, 1993; Dunlop and Özdemir, 1997; Love, 2000). Moreover, volcanic data can yield, in some cases, absolute intensities, while sedimentary data only give relative intensity variation.

A simple method to estimate the PSV comes from calculation of the angular standard deviation (ASD) of virtual geomagnetic poles (VGPs) for a given locality. This method is widely used because there are several models of combination of dipole and non-dipole components that predict the ASD characteristic of PSV as a function of latitude (McFadden *et al*., 1988, 1991). Doell and Cox (1971) and later McWilliams *et al*. (1982) observed, in the zone of the Pacific Ocean around the Hawaii islands, a low angular dispersion of the VGPs during the past 800 kyr or more, and proposed the presence of a low non-dipole field in the central Pacific. Later, Doell and Cox (1972) observed that this low non-dipole field correlates with that calculated from the International Geomagnetic Reference Field (IGRF) for 1945 for the western and central parts of Mexico, and suggested that the low non-dipole field anomaly of central Pacific ex-

*At sabbatical Departamento de Geología y Mineralogía, Universidad Michoacana San Nicolás de Hidalgo.

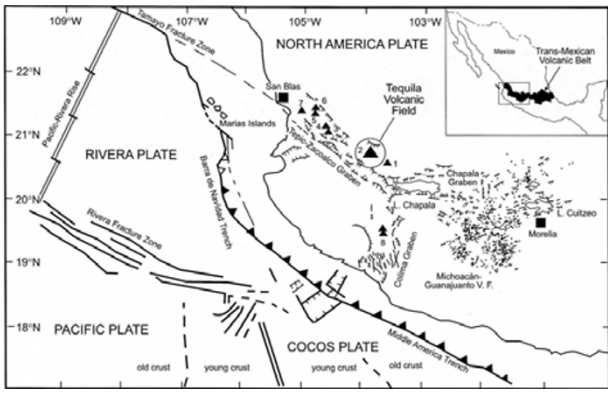

Fig. 1. Tectonic framework of western Mexico, modified from Lewis-Kenedy (2005). Triangles in the Tepic-Zacoalco and Colima grabens refer to main volcanoes: 1. Sierra La Primavera, 2. Tequila, 3. Ceboruco, 4. Tepetitlic, 5. Sanganguey, 6. Las Navajas, 7. San Juan, 8. Colima.

tended to this region (including the Trans-Mexican volcanic belt). The U.S.-Japan Paleomagnetic Cooperation Program in Micronesia (1975) supported this conclusion and considered that a global belt of low average angular dispersion encircles the Earth between 0° and 40° north. Steele (1985) and Herrero-Bervera *et al*. (1986) tested this conclusion for recent part of Brunhes chron. They investigated the PSV for central Mexico from recent volcanic rocks and concluded than the ASD was in agreement with the value predicted from PSV model and that Mexico was not part of low non-dipole field. Bohnel *et al*. (1990) revised this conclusion and found the PSV for central Mexico lower than the PSV models, similar to the value for Hawaii and that the difference with the study of Herrero-Bervera *et al*. (1986) was due to the selection criteria applied to the data set (Urrutia-Fucugauchi, 1997).

The fact that volcanic rocks recorded reversals of the geomagnetic field was already known since David Brunhes's (1907) pioneering contributions. The geomagnetic polarity time scale (GPTS) is now precisely determined for at least the last 160 Myr (Opdyke and Channell, 1996; Berggren, 1995; Harland *et al*., 1990; Cande and Kent, 1992, 1995). The polarity changes and excursions however, for the last 1 Myr is still a matter of debate (Petronille *et al*., 2005). Already Cox (1968) predicted that there should be numerous undiscovered geomagnetic events (excursions or shorter reversed intervals) within Brunhes chron. The most recent Geomagnetic Instability Time Scale (GITS, proposed by Singer *et al*., 2002 to describe geochronology of excursions) shows evidences for 14 geomagnetic excursions in the Brunhes. However, only five (Laschamps, Blake, Jamaica, Calabrian Ridge and Big Lost) are documented by paleomagnetic and high resolution geochronology studies using volcanic rocks.

Both PSV and GITS studies are limited when the age of studied units is poorly constrained. This is the case of central and western Mexico volcanics. Although many studies have been devoted to these crucial problems (see the recent compilation by Mejia *et al*., 2005) and about 200 paleomagnetic directions are available for the last 2 Myr, only few sites were dated directly. In this study, we report a detailed rock-magnetic and paleomagnetic investigation of lava flows associated with Tequila Volcanic Field (TVF) in the Trans-Mexican Volcanic Belt. These sites were recently dated by means of state-of-the-art ^{40}Ar-^{39}Ar method (Lewis-Kenedy *et al*., 2005) and their ages span from 1130 to 150 ka.

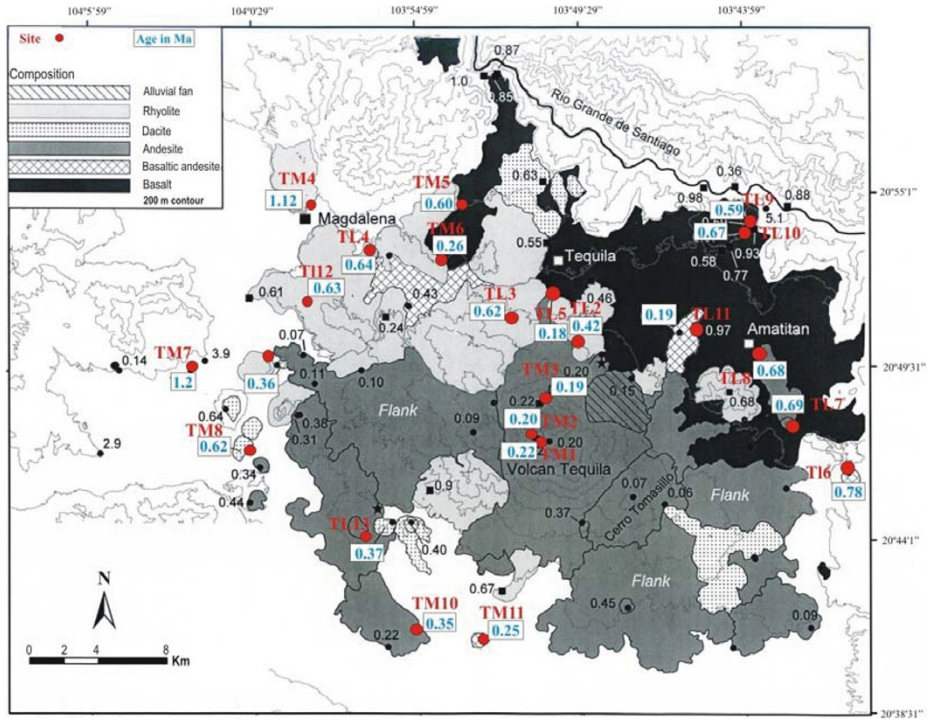

Fig. 2. Simplified geologic map of the TVF and surrounding areas with locations of sampling sites (red dots) and ages (figures within boxes) (modified from Lewis-Kenedy *et al*., 2005).

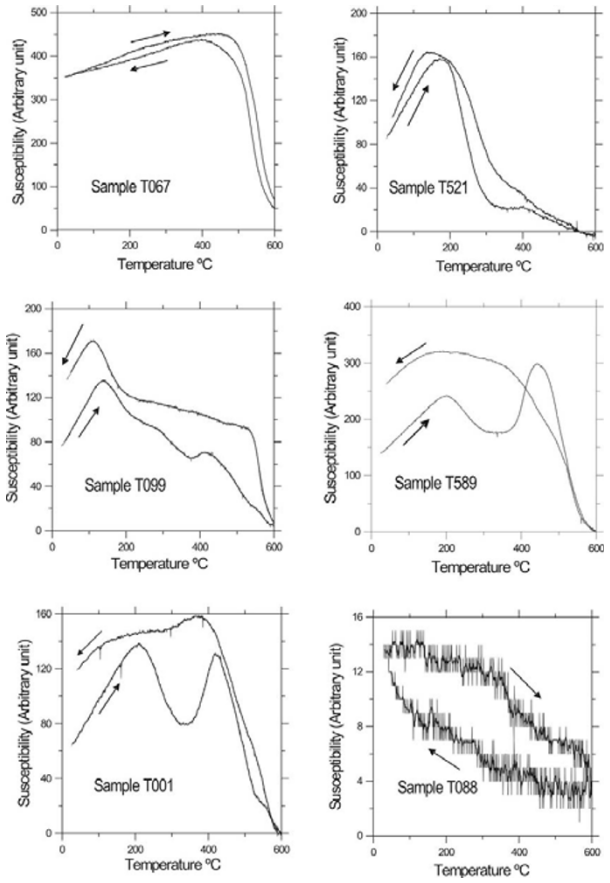

Fig. 3. Susceptibility versus temperature (in air) curves of representative samples. The arrows indicate the heating and cooling curves.

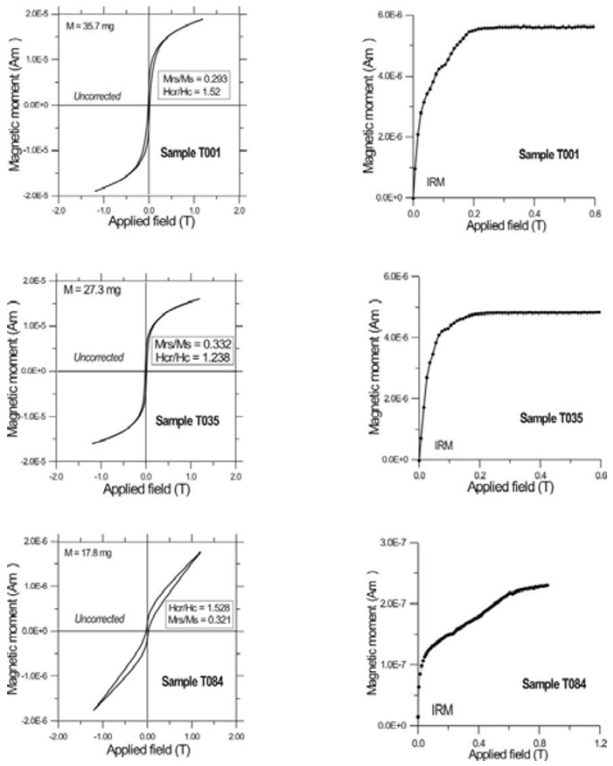

Fig. 4. Typical examples of hysteresis loops (uncorrected) and associated isothermal remanence acquisition curves of small chip samples from the studied volcanic flows. The unit for magnetic moment is Am^2.

2. Location, Ages and Sampling

The Trans-Mexican Volcanic Belt is one of the largest continental volcanic arcs of the North American plate spanning about 1000 km from the Pacific to the Gulf of Mexico (Fig. 1). It is composed of stratovolcanoes, cinder cone fields and silicic caldera complexes. Volcanism has occurred in this region since the late Miocene and it is related to subduction of Cocos and Rivera plates along the Middle America trench. The western part of the belt is associated with subduction of ∼9 Ma Rivera plate, whereas to the east the 12–18 Ma Cocos plate subducts under North America (Klitgord and Mammerickx, 1982). Volcan Tequila is located within the Tepic-Zacoalco graben of western Mexico, one of three grabens that intersect 50 km south-southwest of Guadalajara (Lewis-Kenedy *et al.*, 2005). The andesitic stratocone of Tequila forms the center of the 1600 km^2. TVF is surrounded by rhyolitic domes, flanking andesite flows, cinder cones, and to the north, the Santa Rosa basaltic plateau (Fig. 2).

The eruptive history of the TVF was recently obtained by Lewis-Kenedy *et al.* (2005) using ^{40}Ar-^{39}Ar systematics. New ages were obtained for 49 volcanic units, including Volcn Tequila and surrounding domes, lava flows and cinder cones (Fig. 2). Our sampling strategy was largely conditioned by Lewis-Kenedy *et al.*'s (2005) recent study. We sampled only sites with available isotopic dating information (Fig. 2), easy to access and yielding fresh, apparently not altered outcrops. In total, 188 oriented samples belonging to 24 individual cooling units (Table 1 and 2) were collected. The samples were distributed throughout each flow both horizontally and vertically in order to minimize effects of block tilting. All lava flows sampled were horizontal (dip less than 4°). In general, samples were obtained at the very bottom of flows with the hope of collecting samples with the finest grains of material. Cores were sampled with a gasoline-powered portable drill, and then oriented in most cases with both magnetic and sun compasses.

3. Magnetic Measurements

3.1 Curie points and thermal stability of samples

Low-field susceptibility measurements (k-T curves) under air were carried out using both Highmoore and Bartington susceptibility systems equipped with furnace. One sample from each site was heated up to about 630°C (sometimes to 650°C) at a heating rate of 10°C/min and then cooled at the same rate. Curie temperature was determined by the Prévot *et al.*'s (1983) method.

Five different types of behavior were detected: Twelve sites (Table 2) show the presence of a single magnetic phase with Curie point compatible with relatively low-Ti titanomagnetite (Fig. 3, sample T067). However, in some cases, the cooling and heating curves are not perfectly reversible. In one case (site TM3) the main magnetic carrier seems to be Ti-rich titanomagnetite yielding a Curie point about 240°C (Fig. 3, sample T521). The co-existence of both Ti-poor and Ti-rich titanomagnetites (Sample T099, Fig. 3) is detected for 5 sites (TL5, TL13, TM2, TM6, TM9). Sites TL1, TL4, TL12, TM1 and TM10 show the presence of two ferrimagnetic phases during heating (Fig. 3, samples T001

Table 1. Summary of rock-magnetic parameters for the TVF samples (see also text).

Site	Samples hysteresis and susc. vs T	H_c (mT)	M_{RS} (μAm^2)	M_S (μAm^2)	M_{RS}/M_S	H_{CR} (mT)	H_{CR}/H_C	Mass (mg)	Curie Temperatures					Extimated magnetic mineral
									Heating			Cooling		
									T_{C1}	T_{C2}	T_{C3}	T_{C1}	T_{C2}	
TL1	T001	16.5	4.22	14.4	0.293	25.08	1.52	35.7	260	472	575	500		Titanomaghemite
TL2	T016	13.5	0.489	3.65	0.134	28.69	1.53	20.4	526			530		Ti-poor Titanomagnetite
TL3	T019 T020	9.80	0.907	7.99	0.114	27.78	2.83	28.8	574			570		Ti-poor Titanomagnetite
TL4	T034 T029	21.5	3.94	21.8	0.180	42.233	0.509	34.1	402	570		571		Titanomaghemite
TL5	T035 T039	16.2	3.94	11.9	0.332	20.054	1.238	27.3	270	494		342	548	Ti-rich Titanomagnetite and Ti-poor Titanomagnetite
TL6	T043	25.3	0.400	1.06	0.377	38.66	1.528	14.1	473			542		Ti-poor Titanomagnetite *Low magnetic signal
TL7	T056	9.26	5.09	45.8	0.111	16.616	1.79	24.8	558			560		Ti-poor Titanomagnetite
TL8	T059 T060	5.96	1.77	18.9	0.093	10.964	1.84	13.5	520			512		Ti-relatively poor Titanomagnetite
TL9	T072 T067	16.9	7.92	35.7	0.222	28.542	1.68	20.7	544			532		Ti-poor Titanomagnetite
TL10	T074 T081	8.71	4.54	45.7	0.099	18.35	2.11	20.6	516			436		Ti-relatively poor Titanomagnetite
TL11	T084 T088	33.2	0.170	0.530	0.321	423.97	12.77	17.8						N. D. (low magnetic signal)
TL12	T094 T097	6.61	0.408	5.10	0.080	18.709	2.83	32.2	390	550		542		Titanomaghemite
TL13	T100 T099	15.9	3.16	10.2	0.312	23.532	1.48	26.1	326	494		154	562	Ti-rich Titanomagnetite and Ti-poor Titanomagnetite
TM1	T506 T500	15.5	1.4	6.15	0.228	24.80	1.6	30.3	236	500		538		Titanomaghemite
TM2	T518 T513	10.1	2.48	17.8	0.139	17.99	1.78	33.4	246	512		272	550	Ti-rich Titanomagnetite and Ti-poor Titanomagnetite
TM3	T520 T521	18.5	1.21	5.52	0.218	40.142	2.17	14.5	236			262		Ti-rich Titanomagnetite
TM4	T533	11.6	0.985	8.92	0.110	30.245	2.61	34.5	568			572		Ti-poor Titanomagnetite
TM5	T543 T540	20.2	1.76	8.09	0.217	36.819	1.82	25.2	550			552		Ti-poor Titanomagnetite
TM6	T547	13.8	3.5	15.3	0.228	24.87	1.80	24.8	180	540		170	554	Ti-rich Titanomagnetite and Ti-poor Titanomagnetite
TM7	T557 T561	8.66	1.99	16.6	0.120	21.077	2.43	28.8	550			530		Ti-poor Titanomagnetite
TM8	T568 T567	13.0	3.19	18.2	0.175	24.04	1.85	27.4	544			564		Ti-poor Titanomagnetite
TM9	T577 T581	7.50	2.26	19.9	0.114	15.796	2.106	28.5	224	500		230	504	Ti-rich Titanomagnetite and Ti-poor Titanomagnetite
TM10	T591 T589	14.8	2.41	8.37	0.288	19.94	1.35	21.5	248	512		506		Titanomaghemite
TM11	T602 T596	23.8	5.13	14.9	0.344	37.908	1.59	22.0	530			536		Ti-poor Titanomagnetite

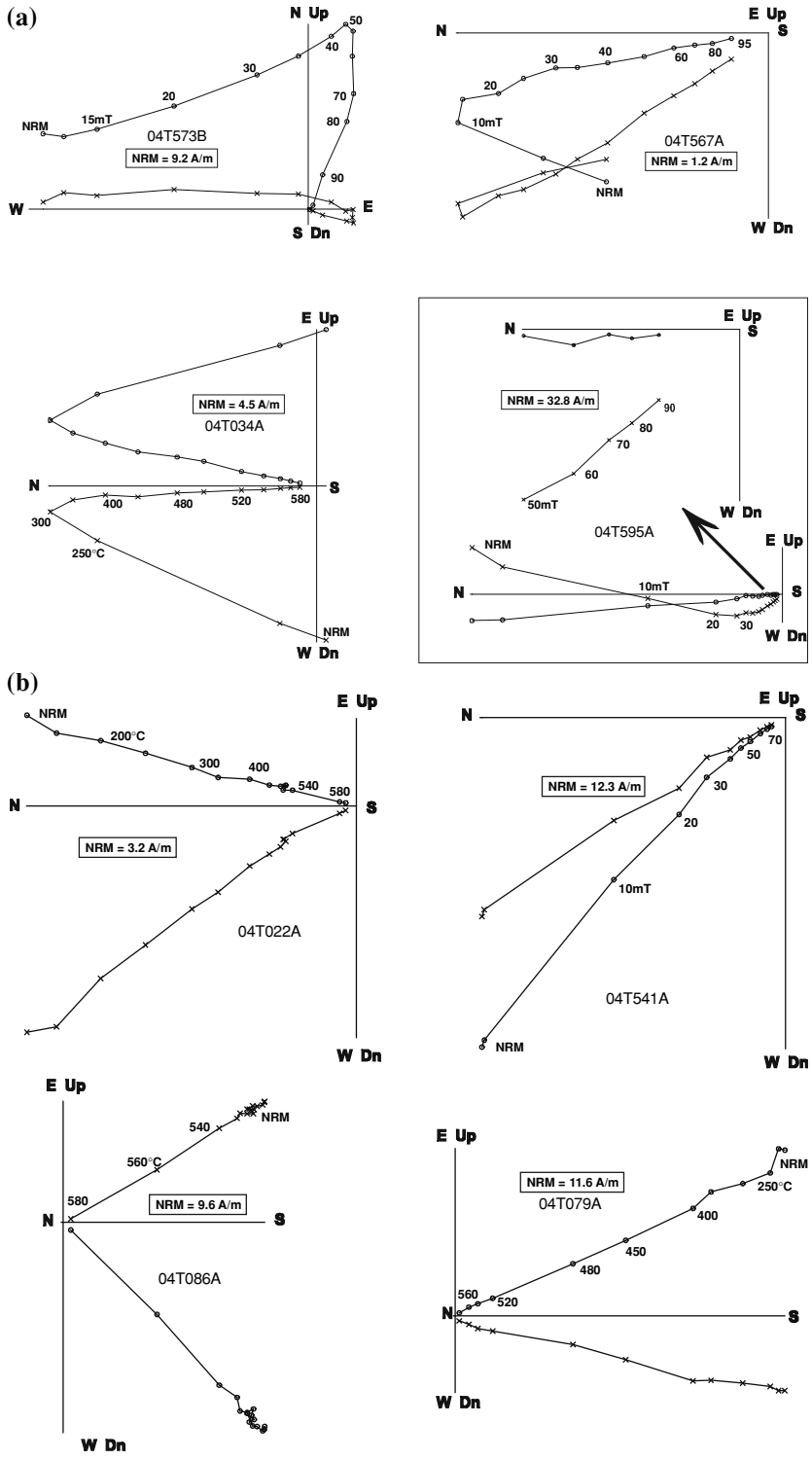

Fig. 5. Orthogonal vector plots of stepwise thermal or alternating field demagnetization of representative samples. The numbers refer either to the temperatures in °C or peak alternating fields in mT. dots—projections into the horizontal plane, crosses—projections into the vertical plane. a) Examples of samples containing strong secondary magnetization components, b) Examples of samples containing univectrorial remanent magnetizations.

and T589). The cooling curve shows only a single phase, with a Curie temperature close to that of magnetite. Such irreversible k-T curves can be explained by titanomaghemite, which probably transformed into magnetite. No correct curve was obtained for the sample T088 (site TL11) because of low initial signal of magnetic susceptibility.

3.2 Hysteresis and IRM experiments

Hysteresis measurements at room temperature were performed on one sample for each studied lava flows using the AGFM 'Micromag' apparatus. in fields up to 1.2 Tesla. These measurements have allowed the determination of saturation magnetisation, M_s, saturation of remanence, M_{rs} and coercivity, H_c. Samples were given an IRM, their mag-

Table 2. Flow-mean paleodirections of cleaned remanence and available isotopic age determinations (Lewis-Kenedy *et al.*, 2005) for the TVF volcanics. N, number of treated samples; n, number of specimens used for calculation; Inc, Inclination; Dec, Declination; k and α_{95}: precision parameter and radius of 95% confidence cone of Fisher statistics, δD: angular distance from the overall mean direction of cleaned remanence. $P_{\rm lat}/P_{\rm long}$: Latitude/Longitude of VGP position, Pol: Magnetic polarity.

Site	Lithology	Geographic		Age	n/N	Inc	Dec	α_{95}	k	δD	$P_{\rm lat}$	$P_{\rm long}$	P_o
		Latitude (N)	Longitude (W)	(Ka)		(°)	(°)	(°)		(°)	(°)	(°)	
TL1	Andesites	20°49.26	103°47.79	115 ± 18	6/8	23.3	358.5	7.7	78	6.33	81.5	86.5	N
TL5	Andesites	20°51.96	103°50.42	178 ± 8	3/7	22.9	359.7	8.8	56	6.71	81.4	78.5	N
TM3	Andesites	20°48.60	103°50.70	191 ± 13	6/8	26.1	10.5	6.5	128	10.6	77.9	16.7	N
TM2	Andesites	20°47.41	103°51.08	196 ± 8	5/8	41.5	345.6	8.9	61	16.2	76.2	183.4	N
TM1	Andesites	20°47.38	103°50.96	216 ± 11	6/9	24.7	12.3	9.9	45	12.6	76.0	17.1	N
TM6	Basalts	20°53.03	103°53.96	261 ± 11	5/7	37.3	11.5	9.6	64	12.8	79.2	342.7	N
TM11	Basaltic andesites	20°41.10	103°52.79	343 ± 38	6/8	48.1	356.4	8.7	63	18.6	80.7	236.6	N
TM10	Andesites	20°41.34	103°55.06	354 ± 15	3/7	33.3	290.5	14.5	23	57.6	24.9	177.7	I
TM9	Basaltic andesites	20°49.75	103°59.69	362 ± 13	9/12	5.8	23.3	6.2	222	32.9	61.3	21.1	I
TL13	Dacites	20°44.85	103°55.82	374 ± 11	0/8	—	—	—	—	—	—	—	X
TL2	Rhyolites	20°50.46	103°49.66	416 ± 3	6/9	20.5	341.6	8.5	63	18.3	69.7	140.0	N
TL9	Basalts	20°53.99	103°43.71	592 ± 20	1/8	9.2	342.3	—	—	25.8	66.6	126.2	N?
TM5	Rhyolites	20°54.76	103°53.44	604 ± 3	7/9	24.3	339.7	9.4	84	18.2	69.1	147.6	N
TM8	Dacites	20°47.00	103°00.46	619 ± 8	6/7	26.9	356.5	7.6	79	3.6	82.9	104.7	N
TL3	Rhyolites	20°51.26	103°51.86	622 ± 3	7/9	17.5	356.7	9.5	82	12.3	78.0	92.4	N
TL6	Basaltic andesites	20°46.23	103°40.52	625 ± 60	0/8	—	—	—	—	—	—	—	X
TL12	Rhyolites	20°51.81	103°58.65	632 ± 8	4/8	20.5	342.6	14.2	33	17.6	70.5	138.3	N
TL4	Rhyolites	20°53.42	103°56.60	642 ± 6	5/8	26.8	1.6	11.5	53	3.8	83.5	62.7	N
TL10	Basalts	20°53.88	103°44.18	671 ± 13	8/8	21.4	164.1	6.4	107	53.1	−54.7	284.3	I
TL8	Andesites	20°50.30	103°43.50	683 ± 32	0/8	—	—	—	—	—	—	—	X
TL7	Andesites	20°47.68	103°42.43	691 ± 26	6/8	39.4	344.1	8.7	52	15.8	75.1	176.7	N
TL11	Basalts	20°50.85	103°45.45	949 ± 68	8/8	−28.2	208.6	8.3	122	25.7	−62.2	173.3	R
TM4	Rhyolites	20°54.80	103°58.50	1121 ± 149	5/9	−45.7	207.7	10.6	65	27.5	−63.9	146.4	R
TM7	Basaltic andesites	20°49.60	104°02.60	1130 ± 159	4/8	−16.9	178.6	13.8	80	12.7	−78.1	262.7	R

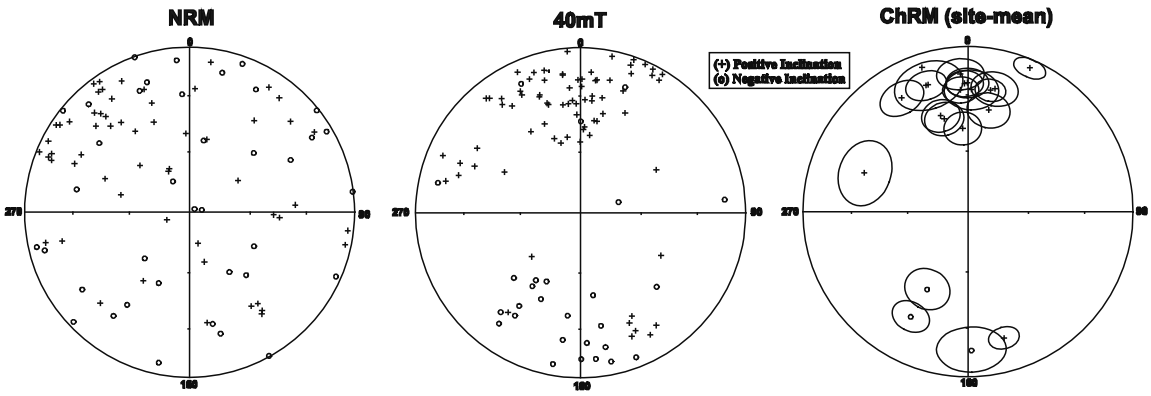

Fig. 6. a) Equal area projections of the natural remanent magnetization, b) idem after application of 40 mT peak alternating fields, c) the flow-mean characteristic paleodirections for the TVF. Crosses/open dots refer to positive/negative inclination.

netisation measured, and then the backfield IRM was applied, giving an indication of the coercivity of remanence, H_{cr}. Combining hysteresis, backfield IRM, coercivity and saturation data allows estimate the bulk magnetic grain size. Some typical hysteresis plots are reported in Fig. 4. Near the origin, no potbellied/wasp-waisted behaviors (Tauxe *et al.*, 1996) were detected, which probably reflects very restricted ranges of the opaque mineral coercivities (samples T001 and T035, Fig. 4). Only exception is site TL11 (Fig. 4 and Table 1, sample T084), yielding a clear wasp-waisted loop. This may reflect the presence of ferrimagnetic phases with different coercivities. Most probably this behavior is due to presence of dominantly single domain and superparamagnetic grains (Goguitchaichvili and Prévot, 2000). It is also possible that this behavior is due to mixture of magnetite and hematite since no saturation of isothermal reme-

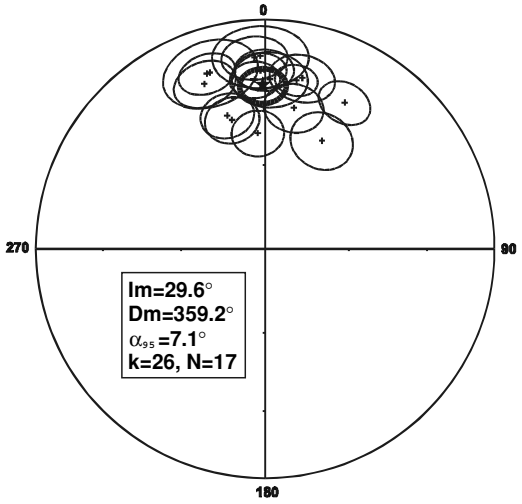

Fig. 7. Equal area projection of the site-mean ChRMs. Reverse polarities are transformed to normal; intermediate polarity are discarded.

nence is reached at about 1 Tesla (Fig. 4). Except this single site, all samples seems to contain 'small' pseudo-single-domain grains judging from hysteresis parameters values (Day *et al*., 1977; Dunlop, 2002). Corresponding isothermal remanence acquisition curves (Fig. 4) were found also very similar for all samples. Saturation is reached in moderate fields of the order of 100–200 mT, which points to some ferrimagnetics as remanence carriers.

3.3 Magnetic treatments

The remanent magnetization of seven to twelve samples from each unit was measured with a JR6 spinner magnetometer (nominal sensitivity $\sim 10^{-9}$ Am^2) installed in shielded room. Both alternating field (AF) and stepwise thermal demagnetization were carried out using a molspin AF-demagnetizer and ASC furnace respectively. During thermal demagnetization, the low-field susceptibility at room temperature was measured after each step with a Bartington susceptibility meter.

At least two magnetization components were recognized for most of studied units (Fig. 5(a)). The less stable components are sometimes much stronger than the stable ones. The characteristic components are isolated after applying 400°C or 50 mT peak alternating field. It should be noted that AF treatment were proved to be very efficient. This is illustrated at Fig. 6. NRM (natural remanent magnetization) directions show large dispersion whereas the dispersion at 40 mT step is drastically reduced and close to the ChRM (characteristic remanence magnetization) direction. The origin of the secondary components in most cases seems to be lightnings judging from relatively high NRM intensity and large within site dispersion. We also note that no ChRM directions were obtained from sites TL13, TL6 and TL8.

For remaining sites, relatively small secondary components, probably of viscous origin, were easily removed applying 200°C or 10 mT (Fig. 5(b)). The greater part of remanent magnetization, in most cases was removed at temperatures between 520 and 580°C, which indicate, once again, low-Ti titanomagnetites as responsible for magnetization. The median destructive field (MDF) range mostly from 20 to 50 mT, suggesting pseudo-single domain grains as remanent magnetization carriers (Dunlop and Özdemir, 1997).

The characteristic magnetization direction was determined by the least squares method (Kirschvink, 1980), 4 to 10 points being taken in the principal component analysis. The obtained directions were averaged by volcanic unit and the statistical parameters calculated assuming a Fisherian distribution. The average unit directions are rather precisely determined for 20 sites (Table 2). Most of the α_{95} are less than 10°.

4. Results and Discussion

We consider the characteristic paleomagnetic directions determined in this study to be of primary origin. Thermomagnetic curves show that the remanence is carried in most cases by Ti-poor titanomagnetite, resulting from oxi-exsolution of original titanomagnetite during the initial flow cooling, which points to a primary thermoremanent origin of magnetization. Some samples seem to contain titanomaghemites as revealed by thermomagnetic analyses. It is possible that these samples carry chemical remanent magnetization related to the low temperature oxidation. However, most of experimental and theoretical studies (Heider and Dunlop, 1987; Özdemir and Dunlop, 1989; Nishitani and Kono, 1989) show that chemical remagnetization by maghemitization have the same direction as the original TRM. Consequently, paleodirections were most probably unaffected by alteration and they can be used for tectonic and magnetostratigraphic application. Moreover, distributed unblocking temperature spectra and relatively high coercivity point to 'small' pseudo-single domain magnetic structure grains as responsible for remanent magnetization.

The characteristic paleodirections are successfully isolated for 20 out of 24 cooling units. No single determination is obtained from sites TL13, TL6 and TL8 and site TL9 is represented by only one sample. These sites as well as transitional (apparently) polarity units (TM10, TM9 and TL10) were discarded from paleomagnetic analysis. The mean paleodirection obtained in this study is $I = 29.6°$, $D = 359.2°$, $k = 26$, $\alpha_{95} = 7.1°$, $n = 17$, which corresponds (Fig. 7) to the mean paleomagnetic pole position $P_{\text{lat}} = 85.8°$, $P_{\text{long}} = 84.3°$, $K = 27.5$, $A_{95} = 6.9°$. These directions are practically undistinguishable from the expected Plesitocene paleodirections, as derived from reference poles for the North American polar wander curve, $D = 355°$; $I = 33.4°$ (Besse and Courtillot, 2002) and in agreement with previously reported directions from Trans-Mexican and Tuxtla Volcanic Belts (Alva-Valdivia *et al*., 2000, 2001; Morales *et al*., 2001). This suggests that no major tectonic deformation occurred in studied area since early-middle Pleistocene to present. Thus, these data may be used for paleosecular variation (PSV) studies.

A simple way to estimate the PSV is to calculate the angular standard deviation ASD of virtual geomagnetic pole for a given locality (McFadden *et al*., 1991). The classic formula $S_F^2 = S_T^2 - S_W^2/n$ was used for estimating paleosecular variation in this study where, here, S_T is the total

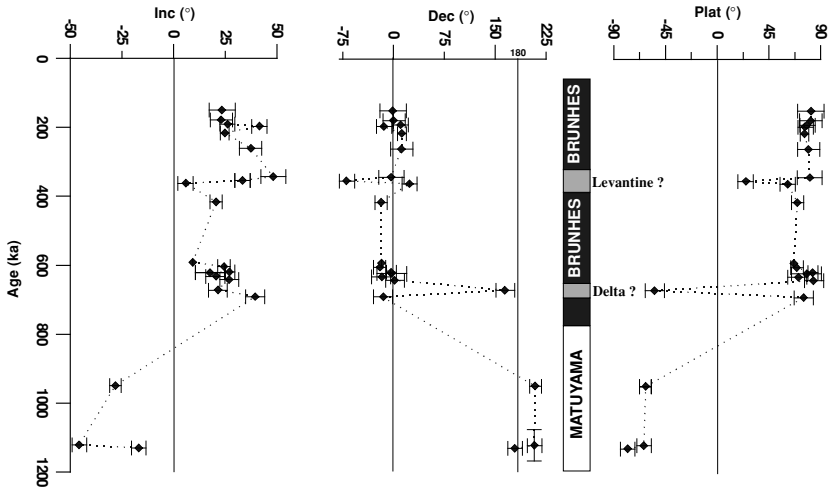

Fig. 8. Flow-mean magnetic inclination, declination and paleolatitude of virtual geomagnetic poles against age.

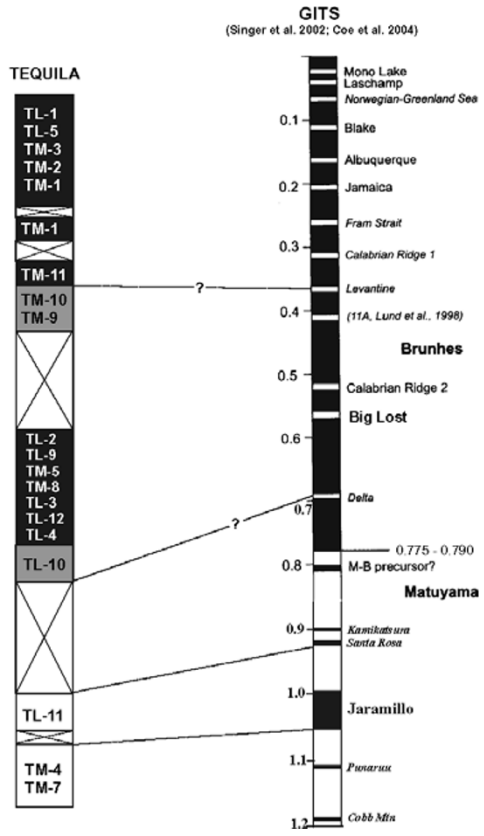

Fig. 9. A tentative correlation between the TVF volcanic units and reference Geomagnetic Instability Time Scale (Singer *et al.*, 2002; Coe *et al.*, 2004).

angular dispersion $S_T = \left[(1/N-1)\sum_{i=1}^{N}\delta i^2\right]^{1/2}$ (Cox, 1969), N the number of sites used in the calculation, δ_i the angular distance of the ith virtual geomagnetic pole from the axial dipole, S_W the within site dispersion and, n the average number of sample per site. Using the new data obtained in this study, we obtained $S_F = 15.4$ with $S_U = 19.9$ and $S_L = 12.5$ (upper and lower limits respectively). The virtual geomagnetic pole scatter is thus consistent with the value predicted by the latitude-dependent variation model of McFadden *et al.* (1988, 1991) for the last 5 Myr. We note here that the calculation of PSV angular dispersion for comparison with the McFadden *et al.* (1991) model requires that the direction are independent in both space and time. It is apparent that each lava flow does not record an independent measurement of the geomagnetic field (see for instance the paleodirections of sites TM3, TM8 and TL3). In this case, samples from several flows that record the same field direction should be averaged together. Directional groups may be defined following Mankinen *et al.*'s (1985) criteria (see also Prévot *et al.*, 1985; Camps and Prévot, 1996). In general, if the flow-mean paleodirections of two or more flows show no systematic trends and their ovals of 95% confidence overlaps, they may be considered to record the same field directions. In our particular case, however, both calculations (using volcanic units or directional groups) gave very similar (statistically indistinguishable) values.

The paleomagnetic declination, inclination and paleolatitude of the VGP (virtual geomagnetic pole) from TVF are shown in Fig. 8 against their stratigraphic position. The oldest sites analyzed (TM7, TM4 and Tl11), all yields reverse polarity magnetizations as expected for the units belonging the Matuyama chron (Figs. 8 and 9). The interesting feature of the record comes from the lava flow TL10 dated as 671 ± 13 ka and yielding clearly defined transitional directions. The choosing of cut-off angle to separate the intermediate and paleosecular variation regime is still a mater of debate. In this study we formally consider the combination of two parameters: the paleodirections are considered intermediate if the latitude of the corresponding VGP is lower than 60° or angular distance from the mean directions exceeds 30°. Thus, intermediate polarity flow TL10 may correspond the worldwide observed Delta excursion at about 680–690 ka yielding first volcanic evidence of this event. The Delta event was first reported from a sediment core in Calabria (Creer *et al.*, 1980) judging from inclination minimums. Champion *et al.* (1981) dated the event to be 630–640 ka using 730 ka for the Brunhes/Matuyama boundary. More recent investigations (Biswas *et al.*, 1999) places Delta event at about 690 ka. Carcaillet *et al.* (2004) found three VDM (virtual dipole moment) minima between

750 and 500 ka, the oldest (about 700 ka) being identified as Delta excursion.

All remained units which correspond to Brunhes chron are normally magnetized (Figs. 8 and 9) excepting flows TM9 and TM10 (dated as 362 ± 13 and 354 ± 5 ka respectively) which may be considered as carriers of the intermediate paleodirections (VGP Lat $= 61.3^\circ$ and ASD $= 32.9$ for TM9 and VGP Lat $= 24.9^\circ$ and ASD $= 57.6^\circ$ for TM10). We note however that the directions for the site TM10 is poorly constrained showing relatively high dispersion (Table 2). The most recent Geomagnetic Instability Time Scale (GITS, proposed by Singer *et al*., 2002 to describe geochronology of excursions; See also Knudsen *et al*., 2003) shows evidences for 14 geomagnetic excursions in the Brunhes chron. However, only five (Laschamps, Blake, Jamaica, Calabrian Ridge and Big Lost) are documented by paleomagnetic and high resolution geochronology studies using volcanic rocks. The remaining excursions were obtained from sedimentary records and thus should be considered cautiously. Levantine excursion at about 360 ka (Singer *et al*., 2002) is particularly poorly defined (Ryan, 1972). Torii *et al*. (1974) found fully reversed directions in the Kasuri ash of the Osaka group—apatite in the ash gave fission track ages of 370–380 ka, in agreement with the estimated age of Biwa III (Yaskawa *et al*., 1974). On the other hand, Champion *et al*. (1988) suggested that anomalous declinations seen in a core from Summer Lake by Negrini *et al*. (1988) just above of ash deposit dated at 360–370 ka may also correspond to Levantine. Our data give some new evidences for the reliability of this event. However, much more data from other part of world are needed to make the firm conclusions.

Acknowledgments. This study was supported by CONACYT (grant no 42661) and UNAM-DGAPA (grant no IN-100403). The constructive reviews of Roberto Lanza and Ruben Somoza are highly appreciated. Maria Rodriguez acknowledges the financial support given by ECOS-ANUIES-CONACYT no M05-U01. Manuel Calvo Rathert acknowledges the financial support of projects BU 16/03 and BU 028A06 of the Junta de Castilla y León.

References

Alva-Valdivia, L. M., A. Goguitchaichvili, L. Ferrari, J. Rosas-Elguera, J. Urrutia-Fucugauchi, and J. J. Zamorano-Orozco, Paleomagnetic data from the Trans-Mexican Volcanic Belt: implications for tectonics and volcanic stratigraphy, *Earth Planets Space*, **52**, 467–478, 2000.

Alva-Valdivia, L. M., A. Goguitchaichvili, and J. Urrutia-Fucugauchi, Further Constraints for the Plio-Pleistocene Geomagnetic Field Strength: new results from Los Tuxtlas volcanic field (Mexico), *Earth Planets Space*, **53**(9), 873–881, 2001.

Berggren, W. A., D. V. Kent, C. C. III Swisher, and M. P. Aubry, A revised Cenozoic Geochronology and Chronostratigraphy, in *Geochronology Time Scales and Global Stratigraphic Correlation*, edited by W. A. Berggren, D. V. Kent, M. P. Aubry, and J. Hardenbol, *SEPM Spec. Pub.*, **54**, 130–212, 1995.

Besse, J. and V. Courtillot, Apparent and true polar wander and the geometry of the geomagnetic field over the last 200 Myr, *J. Geophys. Res.*, **107**(B11), doi 1029/2000JB000050, 2002.

Biswas, D. K., M. Hyodo, Y. Taniguchi, M. Kaneko, S. Katoh, H. Sato, Y. Kinugasa, and K. Mizuno, Magnetostratigraphy of Plio-Pleistocene sediments in a 1700-m core from Osaka Bay, Southwestern Japan, short geomagnetic events in the middle Matuyama, early Bruñes chrons, *Paleogeogr. Plaoeclimatol. Paleoecol.*, **148**, 233–248, 1999.

Bohnel, H., J. Urrutia-Fucugauchi, and E. Herrero-Bervera. Paleomagnetic data from central Mexico and their use for paleosecular variation studies, *Phys. Earth Planet. Inter.*, **64**, 224–236, 1990.

Camps, P. and M. Prévot, A statistical model of the fluctuations in the geomagnetic field from paleosecular variation to reversal, *Science*, **273**, 776–779, 1996.

Cande, S. C. and D. V. Kent, A new geomagnetic polarity time scale for the late Cretaceous and Cenozoic, *J. Geophys. Res.*, **97**, 13917–13951, 1992.

Cande, S. C. and D. V. Kent, Revised calibration of the geomagnetic polarity time scale for the Late Cretaceous and Cenozoic, *J. Geophys. Res.*, **100**, 6093–6095, 1995.

Carcaillet, J. T., D. Bourles, and N. Thouveny, Geomagnetic dipole moment and ^{10}Be production rate intercalibration from authigenic ^{10}Be/^{9}Be for the last 1.3 Ma, *Geochem. Geoph., Geosyst.*, **5**(5), doi 1029/2003GC000641, 2004.

Champion, D. E., G. B. Dalrymple, and M. A. Kunz, Radiometric and paleomagnetic evidence for the Emperor reversed polarity event at 0.46 m.y. in basalt lava flows from the eastern Snake River Olain, Idaho, *Geophys. Res. Lett.*, **8**, 1055–1058, 1981.

Champion, D. E., M. A. Lanphere, and M. A. Kunz, Evidence for a new geomagnetic polarity reversal from lava flows in Idaho: Discussion of short polarity reversals in the Brunhes and late Matuyama polarity chrons, *J. Geophys. Res.*, **93**, 11667–11680, 1988.

Coe, R. S., B. S. Singer, M. Pringle, and X. Zhao, Matuyama-Brunhes reversal and Kamikatsura event on Maui: paleomagnetic directions, ^{40}Ar/^{39}Ar ages and implications, *Earth Planet. Sci. Lett.*, **222**, 667–684, 2004.

Cox, A., Lengths of geomagnetic polarity intervals, *J. Geophys. Res.*, **73**, 3247–3260, 1968.

Cox, A., Confidence limits for the precision parameter k, *Geophys. J. R. astr. Soc.*, **18**, 545–549, 1969.

Creer, K. M., P. Readman, and A. M. Jacobs, Paleomagnetic and paleontological dating of a section at Gioia Tauro, Italy: Identification of the Blake event, *Earth Planet. Sci. Lett.*, **50**, 289–300, 1980.

Day, R., M. Fuller, and V. A. Schmidt, Hysteresis properties of titanomagnetites: Grain-size and compositional dependence, *Phys. Earth Planet. Inter.*, **13**, 260–267, 1977.

Doell, R. and A. Cox, Pacific geomagnetic secular variation, *Science*, **71**, 248–254, 1971.

Doell, R. and A. Cox, The Pacific geomagnetic secular variation anomaly and the question of lateral uniformity in the lower mantle, in *The Nature of the Solid Earth*, edited by E. C. Robertson, McGraw-Hill, New York, pp. 245–284, 1972.

Dunlop, D. J., Theory and application of the Day plot (Mrs/Ms versus Hcr/Hc), Theoretical curves and tests using titanomagnetite data, *J. Geophys. Res.*, **107**, doi:10.1029/2001JB000486, 2002.

Dunlop, D. and O. Özdemir, *Rock-magnetism, Fundamentals and Frontiers*, Cambridge University Press, pp. 573, 1997.

Goguitchaichvili, A. and M. Prévot, Magnetism of oriented single crystals of hemo-ilmenite showing self-reversal of thermoremanent magnetization, *J. Geophys. Res.*, **105**, 2761–2781, 2000.

Harland, W. B., R. Amstrong, A. Cox, L. E. Craig, A. G. Smith, and D. G. Smith, *A Geological Time Scale 1989*, Cambridge University press, Oxford, 1990.

Heider, F. and D. J. Dunlop, Two types of chemical remanent magnetization during oxidation of magnetite, *Phys. Earth Planet. Inter.*, **46**, 24–45, 1987.

Herrero-Bervera, E., J. Urrutia-Fucugauchi, A. Martin del Pozzo, H. Bohnel, and J. Guerrero, Normal amplitude Brunhes paleosecular variation at low-latitudes: A paleomagnetic record from the Trans-Mexican Volcani Belt, *Geophys. Res. Lett.*, **13**, 1442–1445, 1986.

Kirschvink, J. L., The least-square line and plane and analysis of paleomagnetic data, *Geophys. J. R. astr. Soc.*, **62**, 699–718, 1980.

Klitgord, K. D. and J. Mammerickx, Northern East Pacific Rise-Magnetic anomaly and bathymetric framework, *J. Geophys. Res.*, **87**, 6725–6783, 1982.

Knudsen, M. F., N. Abrahamsen, and P. Riisager, Paleomagnetic evidence from Cape Verde Islands basalts for fully reversed excursions in the Brunhes Chron, *Earth Planet. Sci. Lett.*, **206**, 199–214, 2003.

Lewis-Kenedy, C. B., R. A. Lange, C. M. Hall, and H. Delgado-Granados, The eruptive history of the Tequila volcanic field, western Mexico: ages, volumes and relative proportions of lava types, *Bull. Volcanol.*, **67**, 391–414, 2005.

Love, J. J., Palaeomagnetic secular variation as a function of intensity, *Philos. Trans. R. Soc.*, **358**, 1191–1223, 2000.

Lund, S.O., G. Acton, B. Clement, M. Hastedt, M. Okada, and T. Williams, Geomagnetic field excursions occurred often during the last million

years, *EOS Trans. AGU*, **78**(14), spring meet. Suppl., S178–S179, 1998.

Mankinen, E. A., M. Prévot, C. S. Grommé, and R. Coe, The Steens Mountain (Oregon) geomagnetic polarity transition 1, Directional history, duration of episodes and rock-magnetism, *J. Geophys. Res.*, **90**, 10393–10416, 1985.

McFadden, P., T. Merrill, and W. McElhinny, Dipole/quadrupole family modeling of paleosecular variation, *J. Geophys. Res.*, **93**, 11,583–11,588, 1988.

McFadden, P., T. Merrill, W. McElhinny, and S. Lee, Reversals of the Earths magnetic field and temporal variations of the dynamo families, *J. Geophys. Res.*, **96**, 3923–3933, 1991.

McWilliams, M., R. Holcomb, and D. Champion, Geomagnetic secular variation from ^{14}C dated lava flows on Hawaii and the question of the Pacific non-dipole low, *Phil. Trans. R. Soc. Lond.*, **A306**, 211–222, 1982.

Mejia, V., H. Bohnel, M. A. Ortega-Rivera, J. Lee, and J. Aranda-Gomez, Paleosecular variation and time-averaged field recorded in Late Pliocene-Holocene lava flows from Mexico, *Geochem. Geophys. Geosyst.*, **6**, doi:10.1029/2004GC000871, 2005.

Morales, J., A. Goguitchaichvili, and J. Urrutia-Fucugauchi, A rock-magnetic and paleointensity study of some Mexican volcanic lava flows during the Latest Pleistocene to the Holocene, *Earth Planets Space*, **53**, 839–902, 2001.

Negrini, R. M., K. Verosub, and J. O. Davis, The middle to late Pleistocene geomagnetic field recorded in fine-grained sediments from Summer lake (Oregon) and double Hot Spring (Nevada), USA, *Earth Planet. Sci. Lett.*, **87**, 173–192, 1988.

Nishitani, T. and M. Kono, Effects of low-temperature oxidation on the remanence properties of titanomagnetites, *J. Geomag. Geoelectr.*, **41**, 19–38, 1989.

Opdyke, N. D. and J. E. T. Channell, *Magnetic Stratigraphy*, (ed. Academic Press), 246 pp., 1996.

Özdemir, Ö. and D. J. Dunlop, Chemico-viscous remanent magnetization in Fe_3O_4-γFe_2O_3 system, *Science*, **243**, 1043–1047, 1989.

Petronille, M., A. Goguitchaichvili, B. Henry, L. Alva-Valdivia, J. Rosas-Elguera, M. Rodríguez Ceja, and M. Calvo-Rathert, Paleomagnetism of Ar-Ar dated lava flows from the Ceboruco-San Pedro volcanic field (western Mexico): Evidence for the Matuyama-Brunhes transition precursor and a fully reversed geomagnetic event in the Brunhes chron, *J. Geophys. Res.*, **110**, b08101, doi:10.1029/2004jb003321, 2005.

Prévot, M., E. A. Mankinen, S. Grommé, and A. Lecaille, High paleointensities of the geomagnetic field from thermomagnetic study on rift valley pillow basalts from the mid-atlantic ridge, *J. Geophys. Res.*, **88**, 2316–2326, 1983.

Prévot, M., R. S. Mainkinen, R. Coe, and S. Grommé, The Steens Mountain (Oregon) geomagnetic polarity transition 2. Field intensity variations and discussion of reversal models, *J. Geophys. Res.*, **90**, 10417–10448, 1985.

Ryan, W. B., Stratigraphy of late Quaternary sediments in the eastern Mediteranean, in *The Mediteranean Sea*, edited by D. J. Stanley, pp. 149–169, Dowden, Hutchinson & Ross, Stroudsburg, 1972.

Singer, B. S., M. K. Relle, K. A. Hoffman, A. Battle, C. Laj, H. Guillou, and J. Carracedo, Ar/Ar ages from transitionally magnetized lavas on La Palma, Canary Island, and the geomagnetic instability timescale, *J. Geophys. Res.*, **107**(B11), 10.1029/2001JB001613, 2002.

Steele, K. W., Paleomagnetic constraints on the volcanic history of Iztaccihuatl, *Geofisica Internacional*, **24**, 159–167, 1985.

Tauxe, L., Sedimentary records of relative paleointensity: Theory and practice, *Rev. Geophys.*, **31**, 319–354, 1993.

Tauxe, L., T. A. T. Mullender, and T. Pick, Pot-bellies, wasp-waists and superparamagnetism in magnetic hysteresis, *J. Geophys. Res.*, **95**, 12337–12350, 1996.

Torii, M., S. Yoshikawa, and M. Itihara, Paleomagnetism on the water-laid volcanic ash layers in the Osaka Group, Sennan and Senpoku hills, southwest Japan, *Paleogeophys.*, **2**, 34–37, 1974.

Urrutia-Fucugauchi, J., Comments on "A new method to determine paleosecular variation" by D. Vandamme, *Phys. Earth Planet. Inter.*, **102**, 295–300, 1997.

Yaskawa, K., Reversals, excursions and secular variations of the geomagnetic field in the Brunhes normal polarity epoch, in *Paleolimnology of Lake Biwa and the Japanese Pleistocene*, edited by S. Horie, pp. 77–88, Kyoto University Press, 1974.

M. R. Ceja (e-mail: maria@geofisica.unam.mx), A. Goguitchaichvili, M. Calvo-Rathert, J. Morales-Contreras, L. Alva-Valdivia, J. R. Elguera, J. U. Fucugauchi, and H. D. Granados